

Synthesis, Structure, and Reactivity of Bridging Cyanide Complexes of the Formula

$$[(\eta^5\text{-C}_5\text{R}_5)\text{Re}(\text{NO})(\text{PPh}_3)\text{CN}(\text{Ph}_3\text{P})(\text{ON})\text{Re}(\eta^5\text{-C}_5\text{R}'_5)]^+\text{TfO}^-$$

(R, R' = H, Me)

Gene A. Stark, Atta M. Arif, and J. A. Gladysz*

Department of Chemistry, University of Utah, Salt Lake City, Utah 84112

Received February 28, 1997[Ⓢ]

Reactions of $(\eta^5\text{-C}_5\text{R}'_5)\text{Re}(\text{NO})(\text{PPh}_3)(\text{OTf})$ (**1a/b**, R' = H/Me) and $(\eta^5\text{-C}_5\text{R}_5)\text{Re}(\text{NO})(\text{PPh}_3)(\text{CN})$ (**2a/b**, R = H/Me) in toluene or CH_2Cl_2 give the title complexes (R/R' = H/H (**4a**), Me/H (**4b**), H/Me (**4c**), Me/Me (**4d**)) in 71–91% yields as >99:<1, 99–88:1–12, 95–66:5–34, and 71–60:29–40 mixtures of *SR,RS/SS,RR* diastereomers (pseudo *meso/dl*). Reaction of (*S*)-**1a** and (*R*)-**2a** gives (*RR*)-**4a** (retention)—a diastereomer not formed from the racemates. IR and NMR spectra of **4a–d** are analyzed, especially with reference to the cyanide ligands and charge distribution. Cyclic voltammetry shows pseudoreversible oxidations that become thermodynamically more favorable with increased numbers of pentamethylcyclopentadienyl ligands. A crystal structure of (*SR,RS*)-**4a** shows a slightly bent ReCNRe linkage, bond lengths close to those of related $\text{ReC}\equiv$ and $\text{RC}\equiv\text{NRe}$ compounds, and van der Waals contacts across the bridge. The diastereomers of **4a–d** and linkage isomers **4b,c** do not equilibrate in CDCl_3 (55 °C) or $\text{CHCl}_2\text{CHCl}_2$ (98 °C). The dissociation of **4a,d** to **1a/2a** or **1b/2b** is excluded by unsuccessful trapping experiments involving **1a,b**, **2a,b**, and diallyl sulfide (25–120 °C). However, the diallyl sulfide complex $[(\eta^5\text{-C}_5\text{H}_5)\text{Re}(\text{NO})(\text{PPh}_3)(\text{S}(\text{CH}_2\text{CH}=\text{CH}_2)_2)]^+\text{TfO}^-$ and **2a** react ($\text{CHCl}_2\text{CHCl}_2$, 96 °C) to give **4a** (75–63%; 50:50 *SR,RS/SS,RR*). These data show the cyanide bridges to have exceptional kinetic and thermodynamic stabilities.

Complexes in which cyanide ligands link two transition metals have played a prominent historical role in the development of coordination chemistry, include celebrity molecules such as “Prussian blue”, and continue to attract widespread attention.^{1–7} These investigations are so broad in scope that only a soupçon can be highlighted here.¹ For example, remarkable degrees of metal–metal electronic coupling can be observed across cyanide bridges,² and applications as light-harvesting antennae in the sensitization of TiO_2 -based photovoltaic cells have been developed.³ Very large second-order optical nonlinearities have also been recorded.⁴ Some polymeric complexes give lattices that serve as hosts for inclusion compounds,⁵ and linkage

isomerization has been probed in unsymmetrical systems.^{1b,6} In the biological realm, cyanide toxicity has been linked to cytochrome-*c*-derived Fe(III)–CN–Cu(II) units, as supported by studies with synthetic analogs.⁷

We have had an interest in complexes in which two transition metals are linked by unsaturated, carbon-rich ligands.^{8–10} In particular, we have synthesized a series of complexes in which $\text{C}_4\text{–C}_{20}$ polyalkynyl or cumulenic sp carbon chains tether two chiral rhenium Lewis acids, $[(\eta^5\text{-C}_5\text{Me}_5)\text{Re}(\text{NO})(\text{PPh}_3)]^+$ (**I-Me**).⁹ These exhibit novel redox and charge-transfer phenomena involving the metal termini. We were prompted to extend these studies to related bridging cyanide complexes for several reasons. First, cyanide ligands similarly contain only sp-hybridized atoms. Second, replacing a bridging carbon by nitrogen introduces one more electron, providing a species that is isoelectronic with a reduced C_x complex. Third, efforts to prepare complexes in which C_2 bridges span two **I-Me** fragments have been unsuccessful. We were concerned that such assemblies might be sterically prohibitive and thought this could be more easily probed with approximately

[Ⓢ] Abstract published in *Advance ACS Abstracts*, June 1, 1997.

(1) Current comprehensive reviews of this extensive literature are not available. Some lead references: (a) Coe, B. J.; Meyer, T. J.; White, P. S. *Inorg. Chem.* **1995**, *34*, 3600. (b) Darensbourg, D. J.; Yoder, J. C.; Holtcamp, M. W.; Klausmeyer, K. K.; Reibenspies, J. H. *Inorg. Chem.* **1996**, *35*, 4764. (c) Zhu, N.; Pebler, J.; Vahrenkamp, H. *Angew. Chem., Int. Ed. Engl.* **1996**, *35*, 894.

(2) (a) Scandola, F.; Argazzi, R.; Bignozzi, C. A.; Chiorboli, C.; Indelli, M. T.; Rampi, M. A. *Coord. Chem. Rev.* **1993**, *125*, 283. (b) Zhu, N.; Vahrenkamp, H. *J. Organomet. Chem.* **1994**, *472*, C5.

(3) (a) Amadelli, R.; Argazzi, R.; Bignozzi, C. A.; Scandola, F. *J. Am. Chem. Soc.* **1990**, *112*, 7099. (b) O'Regan, B.; Grätzel, M. *Nature* **1991**, *353*, 737. (c) Argazzi, R.; Bignozzi, C. A.; Heimer, T. A.; Meyer, G. J. *Inorg. Chem.* **1997**, *36*, 2 and references therein.

(4) Laidlaw, W. M.; Denning, R. G.; Verbiest, T.; Chauchard, E.; Persoons, A. *Nature* **1993**, *363*, 58.

(5) (a) Park, K.-M.; Iwamoto, T. *J. Chem. Soc., Dalton Trans.* **1993**, 1875. (b) Yuge, H.; Iwamoto, T. *J. Chem. Soc., Dalton Trans.* **1993**, 2841.

(6) (a) Fronczek, F. R.; Schaefer, W. P. *Inorg. Chem.* **1974**, *13*, 727. (b) Zhu, N.; Vahrenkamp, H. *Angew. Chem., Int. Ed. Engl.* **1994**, *33*, 2090. (c) Bignozzi, C. A.; Chiorboli, C.; Indelli, M. T.; Scandola, F.; Bertolasi, V.; Gilli, G. *J. Chem. Soc., Dalton Trans.* **1994**, 2391.

(7) (a) Scott, M. J.; Holm, R. H. *J. Am. Chem. Soc.* **1994**, *116*, 11357. (b) Scott, M. J.; Lee, S. C.; Holm, R. H. *Inorg. Chem.* **1994**, *33*, 4651.

(8) (a) Brady, M.; Weng, W.; Gladysz, J. A. *J. Chem. Soc., Chem. Commun.* **1994**, 2655. (b) Bartik, T.; Bartik, B.; Brady, M.; Dembinski, R.; Gladysz, J. A. *Angew. Chem., Int. Ed. Engl.* **1996**, *35*, 414. (c) Brady, M.; Weng, W.; Zhou, Y.; Seyler, J. W.; Amoroso, A. J.; Arif, A. M.; Böhme, M.; Frenking, G.; Gladysz, J. A. *J. Am. Chem. Soc.* **1997**, *119*, 775.

(9) (a) Weng, W.; Bartik, T.; Gladysz, J. A. *Angew. Chem., Int. Ed. Engl.* **1994**, *33*, 2199 and references therein. (b) Weng, W.; Bartik, T.; Brady, M.; Bartik, B.; Ramsden, J. A.; Arif, A. M.; Gladysz, J. A. *J. Am. Chem. Soc.* **1995**, *117*, 11922.

(10) Weng, W.; Bartik, T.; Johnson, M. T.; Arif, A. M.; Gladysz, J. A. *Organometallics* **1995**, *14*, 889.

isosteric cyanide bridges. Finally, complexes with $C\equiv CCN$ ligands are known,¹¹ and these studies would provide a foundation for the preparation of higher $(C\equiv C)_nCN$ -bridged species.

The triflate complex $(\eta^5-C_5H_5)Re(NO)(PPh_3)(OTf)$ (**1a**)¹² has previously been shown to react with a variety of nitrogen donor ligands to give adducts of the formula $[(\eta^5-C_5H_5)Re(NO)(PPh_3)(L)]^+ TfO^-$.¹³ Also, the cyanide complex $(\eta^5-C_5H_5)Re(NO)(PPh_3)(CN)$ (**2a**)¹⁴ and MeOTf react to give the methyl isocyanide complex $[(\eta^5-C_5H_5)Re(NO)(PPh_3)(CNMe)]^+ TfO^-$.¹⁵ We wondered whether these two reactivity modes might be married to give the title compounds. As chronicled below, this strategy indeed allows ready access to bridging cyanide complexes with all permutations of the rhenium endgroups **I** and **I-Me₅**. A variety of unusual physical and chemical properties are detailed, including data that show the cyanide bridge to be of exceptional kinetic and thermodynamic stability and not subject to facile linkage isomerization.

Results

Syntheses of Bridging Cyanide Complexes. To fully pursue the above objectives, pentamethylcyclopentadienyl analogs of the cyclopentadienyl complexes **1a** and **2a** were required. The cyanide complex $(\eta^5-C_5Me_5)Re(NO)(PPh_3)(CN)$ (**2b**) had been isolated and characterized earlier.¹⁶ The triflate complex $(\eta^5-C_5Me_5)Re(NO)(PPh_3)(OTf)$ (**1b**) was obtained as a powder of $\geq 97\%$ purity by reaction of the methyl complex $(\eta^5-C_5Me_5)Re(NO)(PPh_3)(CH_3)$ (**3b**)¹⁷ and HOTf in toluene at $-45^\circ C$. Alternatively, **1b** was similarly generated and reacted *in situ*. Both methods have been employed in the cyclopentadienyl series. The latter is particularly convenient with neutral Lewis bases, as cationic products usually precipitate from toluene.

Thus, the triflate complexes **1a** and **1b** were generated *in situ* in toluene. As shown in Scheme 1, the cyanide complexes **2a** and **2b** were then added (1.0 equiv). The samples were kept at room temperature for several hours. Some precipitation occurred, and ³¹P NMR spectra of the supernatants showed that all of the reactions, except that of the two pentamethylcyclopentadienyl complexes **1b** and **2b**, were complete. The latter was gently heated, and workup gave the bridging cyanide complexes $[(\eta^5-C_5R_5)Re(NO)(PPh_3)CN(Ph_3P)(ON)Re(\eta^5-C_5R'_5)]^+ TfO^-$ (**4a-d**) in 71–91% yields as yellow, orange, or tan powders.

Complexes **4a-d** were characterized by microanalysis and NMR (¹H, ¹³C, ³¹P), IR, and UV-vis spectroscopies. Data are summarized in the Experimental Section.

(11) Zhou, Y.; Arif, A. M.; Miller, J. S. *J. Chem. Soc., Chem. Commun.* **1996**, 1881 and references therein.

(12) Merrifield, J. H.; Fernández, J. M.; Buhro, W. E.; Gladysz, J. A. *Inorg. Chem.* **1984**, *23*, 4022.

(13) (a) Dewey, M. A.; Knight, D. A.; Klein, D. P.; Arif, A. M.; Gladysz, J. A. *Inorg. Chem.* **1991**, *30*, 4995. (b) Knight, D. A.; Dewey, M. A.; Stark, G. A.; Bennett, B. K.; Arif, A. M.; Gladysz, J. A. *Organometallics* **1993**, *12*, 4523. (c) Dewey, M. A.; Knight, D. A.; Arif, A. M.; Gladysz, J. A. *Z. Naturforsch., B: Anorg. Chem., Org. Chem.* **1992**, *47*, 1175.

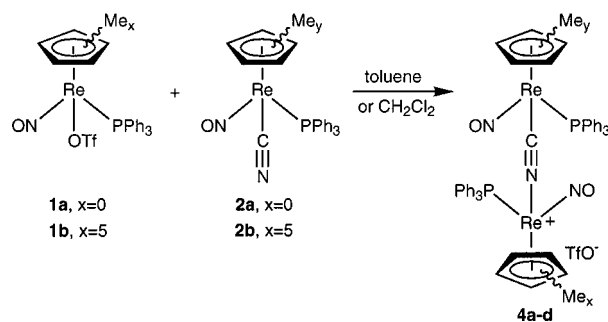
(14) Fernández, J. M.; Gladysz, J. A. *Organometallics* **1989**, *8*, 207.

(15) Richter-Addo, G. B.; Knight, D. A.; Dewey, M. A.; Arif, A. M.; Gladysz, J. A. *J. Am. Chem. Soc.* **1993**, *115*, 11863.

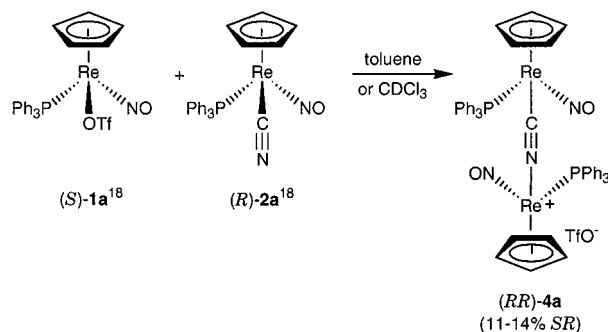
(16) Peng, T.-S.; Winter, C. H.; Gladysz, J. A. *Inorg. Chem.* **1994**, *33*, 2534.

(17) Patton, A. T.; Strouse, C. E.; Knobler, C. B.; Gladysz, J. A. *J. Am. Chem. Soc.* **1983**, *105*, 5804.

Scheme 1. Syntheses of Bridging Cyanide Complexes

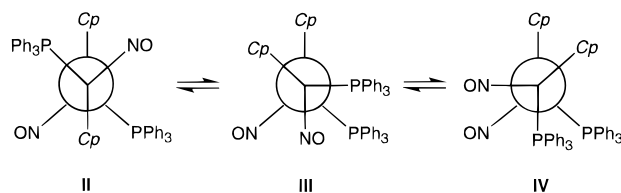


4	x/y	reaction temp (toluene, °C)	isolated yield	SR,RS/SS,RR ratio	SR,RS/SS,RR ratio (CH_2Cl_2 , 40 °C, <i>in situ</i>)
a	0/0	ambient	91%	>99:<1	>99:<1
b	0/5	ambient	86%	99:1	88:12
c	5/0	ambient	84%	95:5	66:34
d	5/5	50	71%	71:29	60:40

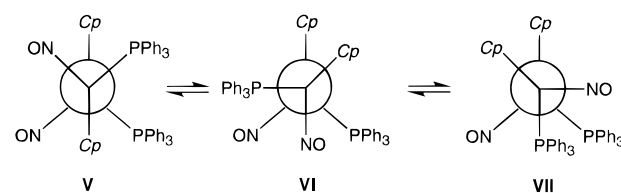


Scheme 2. Conformations of Bridging Cyanide Complexes 4a-d ($Cp = \eta^5-C_5H_5$ or $\eta^5-C_5Me_5$)

SR,RS (SR enantiomer depicted)



SS,RS (SS enantiomer depicted)



Since **4a-d** contain two metal stereocenters, diastereomers are possible, as illustrated in Scheme 2. Attention was given to this issue first. Since the bridging ligand is comprised of two similar atoms and the endgroups are identical or closely related, the diastereomers can be termed pseudo *meso* (SR,RS) and pseudo *dl* (SS,RR).¹⁸ Indeed, ¹H and ³¹P NMR spectra of **4b-d**

(18) (a) Configurations are designated by a modified Cahn-Ingold-Prelog system described earlier.^{13c} Conveniently, the priority sequence $(\eta^5-C_5R_5) > PPh_3 (> OTf) > NO > NCR$ (or CNRe) does not depend upon the ligating atom of the cyanide ligand. (b) The nonracemic compounds in Scheme 1 have configurations opposite to the "default enantiomer" commonly used in this series of papers (PPh_3 switched from right to left, NO switched from left to right).

clearly indicated the presence of two diastereomers (99–71:1–29), as summarized in Scheme 1. Low-temperature ^{31}P NMR spectra ($-100\text{ }^\circ\text{C}$, CH_2Cl_2) did not show any decoalescence or evidence for other types of isomers. However, **4b** and **4c** constitute linkage isomers.

The diastereomer ratios of isolated **4b–d** varied somewhat. Several observations suggested that this might be due to preferential precipitation. Thus, reactions were repeated with isolated **1a** and **1b** under homogeneous conditions in CH_2Cl_2 at $40\text{ }^\circ\text{C}$. These were monitored by ^{31}P NMR, went cleanly to completion, and gave the diastereomer ratios listed in Scheme 1 ($>99\text{--}60\text{:}<1\text{--}40$). Complexes **4a–d** afforded orange to deep red prisms from $\text{CH}_2\text{Cl}_2/\text{hexane}$, which in the case of **4d** were further enriched in the major diastereomer. Thus, some experiments below feature samples of **4b–d** with diastereomer ratios different from those in Scheme 1.

Only one diastereomer of **4a** was detected in all of the above reactions. A crystal structure established an *SR,RS* (pseudo *meso*) configuration. As a check, the opposite diastereomer was independently synthesized. First, the nonracemic triflate complex (*S*)-**1a** was isolated from the reaction of (*R*)- $(\eta^5\text{-C}_5\text{H}_5)\text{Re}(\text{NO})(\text{PPh}_3)(\text{CH}_3)$ (*R*)-**3a**; 97% ee) and HOTf as described earlier.¹² This configurationally labile compound undergoes substitution with a high degree of retention.¹³ As shown in Scheme 1, (*S*)-**1a** and the cyanide complex (*R*)-**2a** ($>98\%$ ee)^{13a,b} were combined in CDCl_3 . The reactants have identical relative configurations,^{18b} as required for a pseudo *dl* product. Accordingly, ^1H and ^{31}P NMR spectra showed the formation of a *new* diastereomer and a small amount of the pseudo *meso* diastereomer (86:14 *RR/SR*). A preparative reaction in toluene gave **4a** in 85% yield as a 89:11 *RR/SR* mixture.

Conformers of the diastereomers of **4a–d** are illustrated in Scheme 2. We had expected, simplistically, that the pseudo *meso* (*SR,RS*) diastereomers would be more stable. Note that in conformation **II** of (*SR,RS*)-**4a**, both the bulky PPh_3 ligands and medium-sized cyclopentadienyl ligands are *anti*. In the only conformation of (*SS,RR*)-**4a** with *anti* PPh_3 ligands (\sim **VI**), the cyclopentadienyl ligands are *gauche*. Thus, by analogy to **4a** and in accord with the likely stability order, the major diastereomers of **4b–d** were assigned *SR,RS* configurations. Importantly, diastereoselectivities decrease as methyl groups are added to the cyclopentadienyl ligands (Scheme 1). As the sizes of the PPh_3 and cyclopentadienyl ligands become similar, energy differences between diastereomers should diminish and rates of formation should be more comparable. As detailed below, efforts to equilibrate diastereomers have been unsuccessful. Hence, the ratios obtained in CH_2Cl_2 are kinetically controlled.

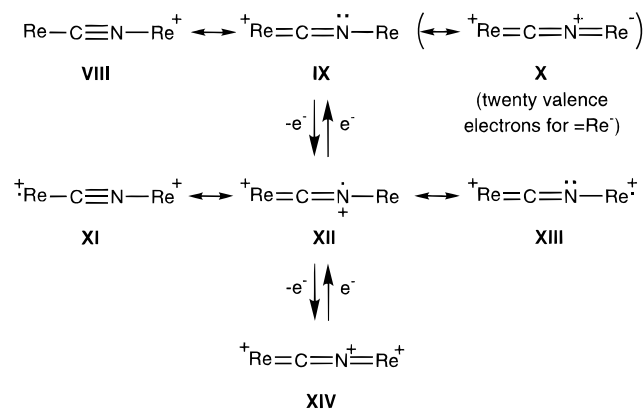
NMR, IR, and UV–Vis Spectra. The bridging cyanide ligands in **4a–d** exhibited distinctive ^{13}C NMR and IR features, as summarized in Table 1. For example, adducts of the cyclopentadienyl cyanide **2a** (^{13}C NMR 121.5 ppm) gave signals at 148.4–149.5 ppm (**4a,c**) whereas adducts of the pentamethylcyclopentadienyl cyanide **2b** (129.3 ppm) gave signals at 157.3–159.1 ppm (**4b,d**). Thus, a 27–30 ppm downfield shift occurs upon coordination of the second rhenium. Similar ^{13}C NMR trends are found with other Lewis base adducts of **I-Me_x**.¹⁴ The signals are coupled to only one phosphorus, with $^2J_{\text{CP}}$ values (10.6–11.4 Hz) that ap-

Table 1. Selected ^{13}C NMR and IR Data

complex	^{13}C NMR, ReCN ^a (CDCl_3 , ppm) [$^2J_{\text{CP}}$, Hz]	IR ν_{CN}^b (cm^{-1} , KBr) [CH_2Cl_2]	IR ν_{NO}^c (cm^{-1} , KBr) [CH_2Cl_2]
2a ^d	121.5 [11.9]	2091 [2097]	1679 [1686]
2b ^e	129.3 [12.1]	2085 [2087]	1655 [1663]
(<i>SR,RS</i>)- 4a	149.5 [11.4]	2091 [2100]	1689 [1690]
(<i>RR</i>)- 4a	148.4 [11.3]	2085 [2089]	1688 [1707]
(<i>SR,RS</i>)- 4b	159.1 [10.9]	2064 [2063]	1680 [1680]
(<i>SR,RS</i>)- 4c	149.2 [10.9]	2071 [2071]	1665/1707 [1669/1703]
(<i>SR,RS</i>)- 4d	157.3 [10.6]	2083 [2080]	1670 [1691]

^a All resonances are doublets. ^b Strong. ^c Very strong. ^d Data from ref 14. ^e KBr data from ref 16.

Scheme 3. Selected Resonance and Redox Relationships



pear very slightly lower than those of **2a,b** (11.9–12.1 Hz). The IR ν_{CN} values of **4a–d** are also generally lower than those of **2a,b** (2064–2091 vs 2085 and 2091 cm^{-1} , KBr). Curiously, the shifts are largest when the termini are different (**4b,c**).¹⁹ There is also a detectable difference between the diastereomers of **4a**.

In principle, **4a–d** should exhibit two IR ν_{NO} bands. However, as summarized in Table 1, **4a,b,d** gave only a single absorption (1670–1689 cm^{-1} , KBr). Some slight band structure was detectable (KBr), but in no case could the underlying peaks differ by more than 10 cm^{-1} . In contrast, **4c** gave two distinct absorptions (1665, 1707 cm^{-1}), roughly approximating those of the cyanide complex **2a** (1679 cm^{-1}) and cationic acetonitrile complex $[(\eta^5\text{-C}_5\text{H}_5)\text{Re}(\text{NO})(\text{PPh}_3)(\text{NCMe})]^+\text{TfO}^-$ (**5**; 1701 cm^{-1}).^{13b} In **4c**, the less basic cyanide complex (**2a**) is paired with the less acidic rhenium fragment (**I-Me₅**). Hence, **4c** should have the lowest dipole across the ReCNRe linkage. The other complexes should have somewhat more positive ReCNRe centers (increasing IR ν_{NO} values) and less positive ReCNRe centers (decreasing IR ν_{NO} values). Complete charge transfer would give the limiting resonance form **IX** in Scheme 3. Note that in the alternative fully cumulated resonance form **X**, the nitrogen-bound rhenium has 20 valence electrons.

There was a surprising absence of the usual charge effects in the NMR spectra of **4a–d**. For example, the neutral cyanide complex **2a** and cationic acetonitrile complex **5** exhibit cyclopentadienyl ^1H NMR signals at δ 5.25 and 5.58, respectively.^{13b,14} However, (*SR,RS*)- and (*RR*)-**4a** each gave two closely spaced signals (δ 5.05, 5.06; 5.06, 5.07), and the chemical shifts of the four

(19) The IR properties of bridging cyanide complexes or Lewis acid adducts have been extensively analyzed, see: (a) Kristoff, J. S.; Shriver, D. F. *Inorg. Chem.* **1973**, *12*, 1788. (b) Shriver, D. F.; Posner, J. *J. Am. Chem. Soc.* **1966**, *88*, 1672. (c) Darenbourg, M. Y.; Barros, H. L. *J. Am. Chem. Soc.* **1979**, *101*, 3286.

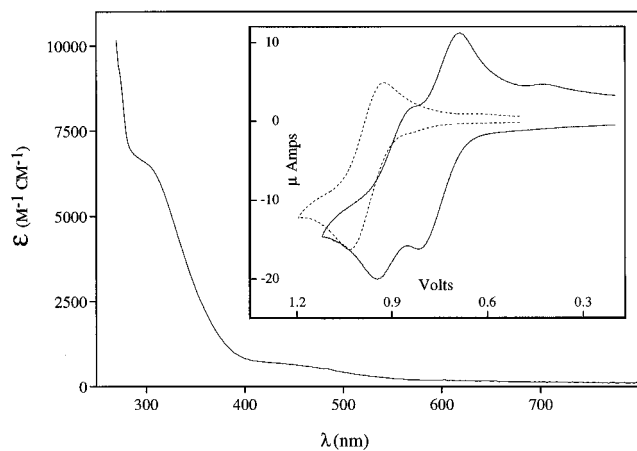


Figure 1. UV-vis spectrum of *(SR,RS)*-**4a** (CH_3CN , ambient temperature, 2.5×10^{-5} M), and (inset) cyclic voltammograms of *(SR,RS)*-**4a** (dashed trace) and **4d** (solid trace, 95/5 *SR,RS/SS,RR*) at 100 mV/s (0.1 M *n*-Bu₄N⁺BF₄⁻/CH₂Cl₂, E° (ferrocene) = 0.46 V).³⁵

cyclopentadienyl ligands of *(SR,RS)*- and *(SS,RR)*-**4b,c** were similar (δ 4.98–5.11; all data in CDCl₃). Analogous, but often less pronounced, relationships are evident throughout other ¹H and ¹³C NMR data in the Experimental Section. For example, the C₅R₅ ¹³C NMR chemical shift ranges were particularly narrow (R = H/Me: 90.7–91.7/101.9–102.4 ppm).

The UV-vis spectra of **4a–d** showed shoulders (302–312 nm, CH₃CN; ϵ 6300–9100 M⁻¹ cm⁻¹) on the intense PPh₃-derived absorption found for all adducts of **I-Me_x**. Extended tails into the visible were also apparent, as illustrated by the representative trace in Figure 1. These may be associated with weak maxima at ca. 400 nm, but this region is obscured by the shoulders. For reference, spectra of **1a**, **2a**, acetonitrile complex **5**, and the benzonitrile complex [(η^5 -C₅H₅)Re(NO)(PPh₃)(NCPH)]⁺ TfO⁻ (**6**)^{13b} were obtained under identical conditions. The benzonitrile complex **6** gave a similar shoulder (314 nm; ϵ 6600 M⁻¹ cm⁻¹) but **1a**, **2a**, and **5** did not.

Other Physical Characterization. We sought to crystallographically confirm the structure of a representative complex. Thus, X-ray data were collected on *(SR,RS)*-**4a** as outlined in Table 2. Refinement afforded the structures shown in Figure 2, verifying the pseudo *meso* diastereomer assignment. There are no close contacts of the cation with the triflate anion. Selected bond lengths and angles are summarized in Table 3.

The N–Re–C, P–Re–C, N–Re–P, and N–Re–N bond angles range from 86° to 100°, consistent with formally octahedral rhenium geometries and the idealized structures **II–VII** in Scheme 2. The ReCNRe linkage is slightly bent, with Re'–C1–N1 and C1–N1–Re bond angles of 173.1(12)° and 174.5(10)°. The Re'–C1 bond length, 2.013(14) Å, may be slightly shorter than those in similar complexes with Re–C≡C–Pd and Re–C≡C–CH₃ moieties (2.079(9), 2.066(7) Å).^{9b,20} The Re–N1 and N1–C1 bond lengths, 2.083(14) and 1.15(2) Å, nearly match those of the related nitrile complex (SS)-[(η^5 -C₅H₅)Re(NO)(PPh₃)(NCCH(Ph)Et)]⁺ PF₆⁻ (2.089(8), 1.131(10) Å),²¹ which also exhibits a slightly bent ReNCC linkage (ReNC 168.5(6)°, NCC 177.9(8)°).

(20) Senn, D. R.; Wong, A.; Patton, A. T.; Marsi, M.; Strouse, C. E.; Gladysz, J. A. *J. Am. Chem. Soc.* **1988**, *110*, 6096.

Table 2. Summary of Crystallographic Data for *(SR,RS)*-**4a**

molecular formula	C ₄₈ H ₄₀ F ₃ N ₃ O ₅ P ₂ Re ₂ S
mw	1262.23
temp of collection, K	291(2)
cryst syst	monoclinic
space group	<i>P</i> 2 ₁ / <i>n</i>
cell dimens	
<i>a</i> , Å	9.7699(12)
<i>b</i> , Å	24.208(11)
<i>c</i> , Å	19.114(3)
β, deg	91.950(13)
<i>V</i> , Å ³	4518(2)
<i>Z</i>	4
<i>d</i> _{calcd} , g/cm ³	1.856
<i>d</i> _{obs} , g/cm ³ (CCl ₄ /CH ₂ I ₂)	1.853
cryst dimens, mm	0.29 × 0.25 × 0.11
diffractometer	Enraf-Nonius CAD-4
radiation, Å	Mo Kα (0.710 73)
data collection method	θ–2θ
scan speed, deg/min	variable
no. of reflns measd	7525
range/indices (<i>h,k,l</i>)	0–11, 0–27, –21 to 21
2θ limit, deg	2.13–23.97
standard reflection check	1 X-ray h
no. of total unique data	7067
no. of obsd data, <i>I</i> > 3σ(<i>I</i>)	6976
abs coeff, cm ⁻¹	55.34
min transmission, %	0.599
max transmission, %	0.999
no. of variables	577
goodness of fit	1.057
R = Σ <i>F</i> _o – <i>F</i> _c /Σ <i>F</i> _o	0.0461
wR2 = (Σ[w(<i>F</i> _o ² – <i>F</i> _c ²) ²]/Σ[w(<i>F</i> _o ⁴)] ^{1/2})	0.0928
Δ <i>σ</i> (max)	0
Δρ (max), e/Å ³	1.239 (1.525 Å from C6)

The ReCNRe conformation places the PPh₃ ligands approximately *anti*. However, the angle between the P'–Re–C1 and N1–Re–P planes (141.0(4)°) is much smaller than in idealized structure **II** in Scheme 2 (180°). Interestingly, while the PPh₃ ligand of one rhenium (Re') is *gauche* with respect to the cyclopentadienyl ligand of the other (Re), the opposite PPh₃/cyclopentadienyl ligands are nearly eclipsed. A slight counterclockwise rotation of the front rhenium in the bottom view in Figure 2 would give a more symmetrical disposition. When the structure is viewed stereoscopically with atoms at van der Waals radii, a cyclopentadienyl proton squarely abuts a PPh₃ phenyl π face in the eclipsed pair. Such interactions are now recognized as attractive²² and were not considered in the analysis of rotamer or diastereomer stabilities in Scheme 2.

Although there is no appreciable van der Waals overlap in *(SR,RS)*-**4a**, there should be marked destabilizing steric interactions in the bis(pentamethylcyclopentadienyl) analog **4d**. The rhenium–rhenium distance, 5.237(2) Å, is the shortest to date for a complex with two **I-Me_x** moieties tethered by a bridging ligand of overall linear geometry. In the previous record holder, **7** (Chart 1), the rheniums are separated by three carbons and 6.1025(6) Å.¹⁰ However, the rhenium–rhenium distance in the bent bridging iodide complex **8** is shorter still (4.526(2) Å).²³

(21) Merrifield, J. H.; Lin, G.-Y.; Kiel, W. A.; Gladysz, J. A. *J. Am. Chem. Soc.* **1983**, *105*, 5811.

(22) (a) Nishio, M.; Umezawa, Y.; Hirota, M.; Takeuchi, Y. *Tetrahedron* **1995**, *51*, 8665. (b) Dance, I.; Scudder, M. *J. Chem. Soc., Dalton Trans.* **1996**, 3755. (c) Brunner, H.; Oeschey, R.; Nuber, B. *Organometallics* **1996**, *15*, 3616 and references therein.

(23) Winter, C. H.; Arif, A. M.; Gladysz, J. A. *Organometallics* **1989**, *8*, 219.

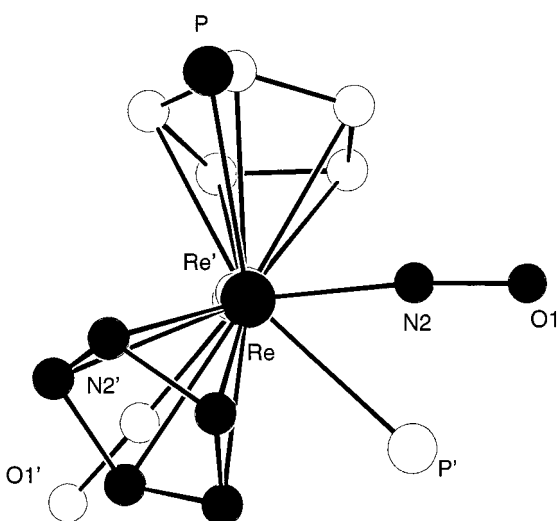
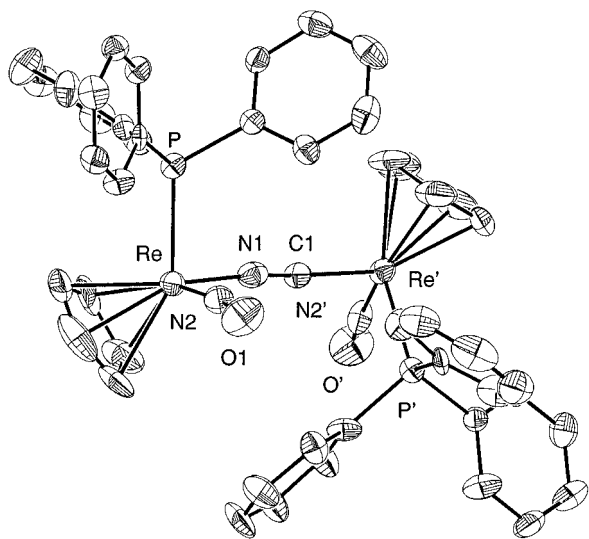


Figure 2. Structure of the cation of *(SR,RS)*-**4a** (top) and Newman-type projection down the rhenium–rhenium axis with phenyl rings omitted (bottom).

Table 3. Key Bond Lengths (Å) and Angles (deg) in *(SR,RS)*-4a****

Re–N(1)	2.083(13)	Re–C(1)	2.013(14)
Re–N(2)	1.757(12)	Re–N(2')	1.768(13)
Re–P	2.386(3)	Re'–P'	2.365(3)
P–C(19)	1.804(13)	P'–C(19')	1.812(13)
P–C(7)	1.832(13)	P'–C(7')	1.82(2)
P–C(13)	1.843(12)	P'–C(13')	1.831(13)
N(2)–O(1)	1.20(2)	N(2')–O(1')	1.198(14)
N(1)–C(1)	1.15(2)	Re–Re'	5.237(2)
Re–N(1)–C(1)	174.5(10)	Re'–C(1)–N(1)	173.1(12)
N(2)–Re–N(1)	96.4(5)	N(2')–Re'–C(1)	100.5(5)
N(2)–Re–P	94.4(4)	N(2')–Re'–P'	90.0(4)
N(1)–Re–P	89.0(3)	C(1)–Re'–P'	86.4(4)
Re–P–C(19)	109.9(4)	Re'–P'–C(19')	116.1(4)
Re–P–C(7)	119.1(4)	Re'–P'–C(7')	113.5(5)
Re–P–C(13)	114.6(4)	Re'–P'–C(13')	114.4(4)
Re–N(2)–O(1)	170.1(12)	Re'–N(2')–O(1')	172.2(12)

Cyclic voltammograms of **4a–d** ($\geq 94:6$ *SR,RS/SS,RR*) were recorded in CH_2Cl_2 , as described in the Experimental Section. Complexes **4a–c** each gave one pseudoreversible (presumably one-electron) oxidation, as summarized in Table 4 and illustrated by the representative trace in Figure 1. The bis(pentamethylcyclopentadienyl) complex **4d** exhibited two closely spaced oxidations ($\Delta E^\circ = 0.13$ V), as well as a small cathodic

Chart 1. Other Relevant Crystallographically Characterized Complexes

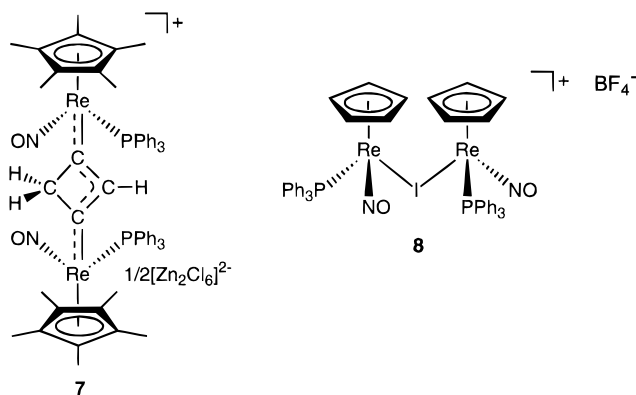


Table 4. Summary of Cyclic Voltammetry Data^a

complex	<i>SR,RS/SS,RR</i> ratio	$E_{p,a}$ [V]	$E_{p,c}$ [V]	E° [V]	ΔE (mV)	I_a/I_c
4a	>99:<1	1.03	0.93	0.98	100	>1
4b	94:6	0.97	0.89	0.93	80	>1
4c	95:5	0.99	0.87	0.90	120	>1
4d	95:5	0.82	0.69	0.75	130	>1
		0.95	0.81	0.88	140	>1

^a Conditions are given in Figure 1 and the Experimental Section.

peak suggestive of an ECE process (Figure 1). As would be expected, oxidations became thermodynamically more favorable with increasing numbers of more electron-releasing pentamethylcyclopentadienyl ligands. The linkage isomers **4b,c** exhibited only slightly different potentials. No reductions were observed out to the solvent-imposed cathodic limit of -1.2 V.

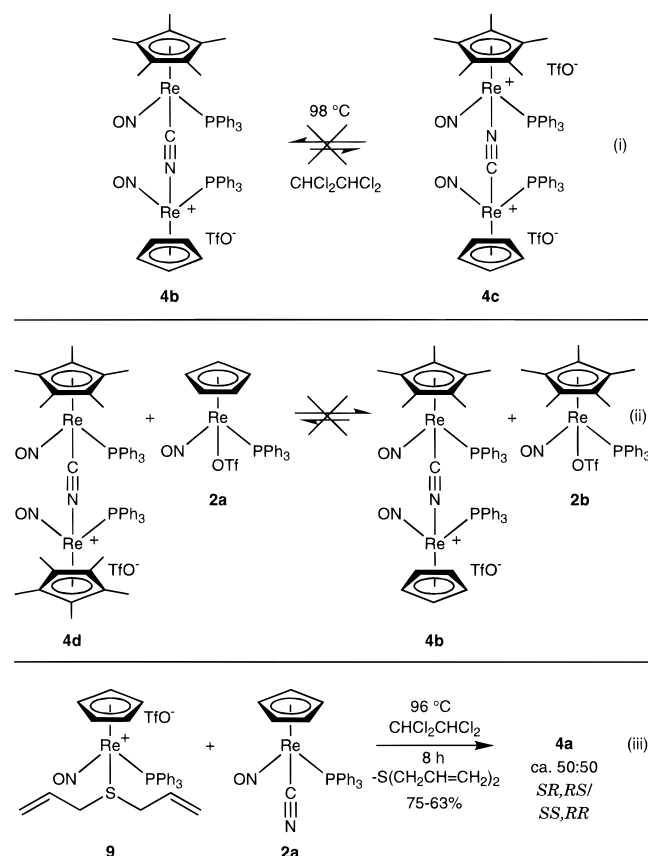
Reactions. We first sought to assay for two thermal processes, diastereomeric equilibria and linkage isomerism. The latter has rarely been observed with bridging cyanide complexes.^{1b,6c} However, many “cyano” and “isocyano” (X–CN , X–NC) species readily interconvert.²⁴ Complexes **4a–d** offer several probes for such isomerism. For example, **4b** and **4c**, which are easily distinguished spectroscopically, would equilibrate (eq i, Scheme 4). On the basis of the relative Lewis acidities of the rhenium fragments **I** and **I–Me₅**, **4b** would be expected to be more stable. Isomerization would also racemize the pseudo *meso* complexes (*SR*)-**4a,d** but would be degenerate for the pseudo *dl* complexes (*RR*)-**4a,d**.²⁵

Thus, CDCl_3 solutions of **4a** (>99:<1 *SR,RS/SS,RR*), **4b** (99:1), **4c** (88:12), and **4d** (71:29) were kept at 55°C for 25 h. There appeared to be very slight changes in the diastereomer ratios of **4b** (97:3) and **4d** (67:33), as assayed by NMR (^1H , ^{31}P). However, the values are close to experimental error, and it is also possible that one diastereomer undergoes a slow independent decomposition. An identical experiment with the opposite

(24) Rüdhardt, C.; Meier, M.; Haaf, K.; Pakusch, J.; Wolber, E. K. A.; Müller, B. *Angew. Chem., Int. Ed. Engl.* **1991**, *30*, 893.

(25) These points can be visualized with the formulae $\text{Re}_S\text{–CN–Re}_R \rightleftharpoons \text{Re}_S\text{–NC–Re}_R$ (pseudo *meso*; linkage isomers and enantiomers),^{18a} and $\text{Re}_S\text{–CN–Re}_S \rightleftharpoons \text{Re}_S\text{–NC–Re}_S$ (pseudo *dl*; identical). We did not attempt to prepare (*SR*)-**4a** and measure a racemization rate, since extensive experiments would have been required to exclude other racemization mechanisms (e.g., equilibria involving configurationally labile **1a**,¹² PPh_3 dissociation²⁶).

(26) Dewey, M. A.; Stark, G. A.; Gladysz, J. A. *Organometallics* **1996**, *15*, 4798 and references therein.

Scheme 4. Other Attempted Reactions Involving 4a–d


diastereomer of **4a** (89:11 *RR/SR*) did give partial decomposition, as evidenced by a black suspension, but with little change in the diastereomer ratio. In no case was any equilibration of **4b** and **4c** detected. A $CHCl_2-CHCl_2$ solution of **4b** (99:1 *SR,RS/SS,RR*) was similarly kept at 98 °C for 12 h (eq i, Scheme 4). Two decomposition products formed (14%) but no **4c** was observed and most of the **4b** remained (86%; 97:3 *SR,RS/SS,RR*). Comparable results were obtained with a $CHCl_2CHCl_2$ solution of **4c**.

As a further check, solid samples of **4a–d** (>99:<1, 99:1, 88:12, 98:2 *SR,RS/SS,RR*) were analyzed by differential scanning calorimetry (DSC). Complex **4a** melted without decomposition at 247 °C. The others thermally decomposed without melting at similar temperatures. There were no indications of any isomerizations or other phase transitions. Hence, **4b** and **4c** do not readily equilibrate in solution or the solid state.

The possibility that a rhenium moiety might dissociate from the bridging cyanide ligand was probed. As noted above, **I** is a stronger Lewis acid than **I-Me₅** and sterically less congested. Therefore, if the bis(pentamethylcyclopentadienyl) complex **4d** were in equilibrium with the precursors **1b** and **2b** (Scheme 1), it would be highly probable that the latter could be trapped by added cyclopentadienyl triflate **1a**. This would give the overall reaction shown in eq ii of Scheme 4. Thus, a CD_2Cl_2 solution of **4d** (98:2 *SR,RS/SS,RR*) and **1a** (1 equiv) was kept at room temperature for 5 days. No reaction was detected by ¹H and ³¹P NMR.

In the event that the anticipated direction of the equilibrium was incorrect, three similar experiments were conducted. First, a $CDCl_3$ solution of **4d** (70:30

SR,RS/SS,RR) and the cyanide complex **2a** was kept at 47 °C for 12 h. No reaction occurred, except for a slight change in the diastereomer ratio (62:38). Second, a $CDCl_3$ solution of (*SR,RS*)-**4a** and the pentamethylcyclopentadienyl triflate **1b** was kept at 58 °C for 12 h. The former did not react, but the latter decomposed to several products. Third, a $CDCl_3$ solution of (*SR,RS*)-**4a** and **2b** were kept at 58 °C for 38 h. The solution turned green, and approximately half of **2b** decomposed. However, no **4b** was detected.

Since the preceding experiments provided no evidence for thermal cleavage of the cyanide bridges in **4a–d**, reactions with nucleophiles were investigated. Diallyl sulfide was studied first, as (1) diallyl sulfide complexes of **I** and **I-Me₅** had been characterized²⁷ and (2) dialkyl sulfides are some of the strongest nucleophiles for displacing dichloromethane from **I**.²⁸ Thus, a $CDCl_3$ solution of (*SR,RS*)-**4a** and diallyl sulfide (2 equiv) was kept at 47 °C for 12 h. No reaction occurred, as assayed by ¹H and ³¹P NMR. Next, a $CDCl_3$ solution of **4d** (70:30 *SR,RS/SS,RR*) and diallyl sulfide was similarly kept at 50 °C for 4 days. No new NMR signals appeared. However, the diastereomer ratio decreased to 51:49. A control showed no independent isomerization of **4d** (73:27 *SR,RS/SS,RR*) under identical conditions, suggesting that the diallyl sulfide promotes diastereomer interconversion.

Next, (*SR,RS*)-**4a** and diallyl sulfide (5 equiv) were combined in the higher boiling solvent $CHCl_2CHCl_2$. After 7 h at 120 °C, a ³¹P NMR spectrum showed that 92% of **4a** had disappeared. Many products formed (43.4, 25.4, 16.5–14.1 ppm; 38:3:51) but no diallyl sulfide complex $[(\eta^5-C_5H_5)Re(NO)(PPh_3)(S(CH_2CH=CH_2)_2)]^+ TfO^-$ (**9**)²⁷ or **2a** was detected. Thus, we checked the possibility that bridge cleavage by diallyl sulfide might not be favored thermodynamically. As shown in eq iii of Scheme 4, a $CHCl_2CHCl_2$ solution of **9** and **2a** (1 equiv) was kept at 96 °C for 8 h. The sample turned black, and ³¹P and ¹H NMR spectra indicated 75–63% yields of **4a**. Hence, **2a** is a stronger base than diallyl sulfide toward **I**. In contrast to the above syntheses of **4a**, nearly equal amounts of the two diastereomers formed. However, no equilibration occurred when the crude isolated sample (43:57 *SR,RS/SS,RR*) or (*SR,RS*)-**4a** were independently kept in $CHCl_2CHCl_2$ at 98 °C.

Cyanide ion displaces many nitrogen donor ligands from **I**.¹³ Thus, (*SR,RS*)-**4a** and $Et_4N^+ CN^-$ (2 equiv) were combined in $CDCl_3$ in the hope of forming **2a** (2 equiv). After 22 h at room temperature, ca. 95% of the (*SR,RS*)-**4a** was consumed. However, a ¹H NMR spectrum showed six cyclopentadienyl signals (δ 5.59, 5.51, 5.46, 5.33 (**2a**), 5.27, 5.00; 2:16:20:46:2:12). A ³¹P NMR spectrum showed eight signals (30.7 (OPPh₃), 17.6 (**2a**), 17.4, 17.3, 16.6, 15.8, 13.8, –4.7 (PPh₃) ppm; 7:46:14:2:3:1:14:13). Although **2a** was the major product (ca. 46% or 1 equiv), more complex processes were clearly operative. Regardless, cyanide ion constitutes the only external agent found to react with **4a–d** at room temperature to date. The rate is much slower than for other nitrogen donor ligand adducts of **I**.¹²

(27) Cagle, P. C.; Meyer, O.; Weickhardt, K.; Arif, A. M.; Gladysz, J. A. *J. Am. Chem. Soc.* **1995**, *117*, 11730.

(28) Dewey, M. A.; Zhou, Y.; Liu, Y.; Gladysz, J. A. *Organometallics* **1993**, *12*, 3924.

Discussion

Scheme 1 establishes that cationic bridging cyanide complexes that are isostructural and isoelectronic with the unknown neutral C_2 complexes $(\eta^5-C_5R_5)Re(NO)(PPh_3)(C\equiv C)(Ph_3P)(ON)Re(\eta^5-C_5R'_5)$ (**10a–d**) are easily isolated. Hence, **10a–d** constitute viable synthetic targets. A higher homolog, $(\eta^5-C_5Me_5)Re(NO)(PPh_3)(C\equiv CC\equiv C)(Ph_3P)(ON)Re(\eta^5-C_5Me_5)$ (**11d**), is easily prepared.^{8c} As with the bis(pentamethylcyclopentadienyl) analog **4d**, **11d** undergoes two successive one-electron oxidations, but at thermodynamically much more favorable potentials (+0.01 and 0.54 vs 0.75 and 0.88 V under the conditions of Figure 1). Due to the shorter chain, **10d** should be oxidized even more readily.^{8b} Thus, the substitution of carbon by a more electronegative, positively charged nitrogen renders oxidation much more difficult. Conversely, reductions should be facilitated, and we had hoped to access redox states that cannot be reached with **11d**. However, the CH_2Cl_2 solvent is reduced first.

The oxidation products of **4a–d** are furthermore much less stable than those of **11d**. The dications would be paramagnetic, mixed-valence compounds.² The odd electrons could potentially be delocalized over both rheniums, as in resonance forms **XI** and **XIII** in Scheme 3. The trication derived from **4d** would have a fully cumulated structure, as in **XIV** (Scheme 3). In an attempt to isolate an oxidized complex, **4a** was methathesized to a hexafluorophosphate salt and treated with $Ag^+ PF_6^-$ (CH_2Cl_2 , room temperature). The solution turned olive green, but the IR bands shifted only slightly. Numerous diamagnetic decomposition products were obtained upon workup. However, other bridging cyanide complexes have proved isolable in more than one oxidation state.^{2b}

The syntheses of **4a–d** have abundant precedent. In general, terminal cyanide complexes are much stronger bases and nucleophiles than organic nitriles and are readily attacked by carbon, protic, and transition metal electrophiles.²⁹ Also, the enantiomers of the chiral iron cyanide complex $(\eta^5-C_5H_5)Fe(CO)(PPh_3)(CN)$ are differentiated by chiral NMR shift reagents to a much greater degree than related iron complexes.³⁰ This pattern holds with the isostructural complex **2a**, suggesting dominant contact shift interactions with the cyanide nitrogens. In this context, **4a–d** are to our knowledge the only bridging cyanide complexes with two chiral-at-metal endgroups. Thus, there is the opportunity for chiral recognition, both in kinetic and thermodynamic contexts.

Unfortunately, we have not been able to obtain equilibrium diastereomer ratios for **4a–d**. Only in the case of the most congested complex, **4d**, do ratios significantly change in solution in the absence of any apparent reaction or decomposition (71:29 to 51:49 and 70:30 to 62:38 *SR,RS/SS,RR*, $CDCl_3$, 50–47 °C, 4.0–0.5 days). Furthermore, this only occurs in the presence of the nucleophiles diallyl sulfide or **2a**. A possible rationale is offered below. As analyzed above, the *SR,RS* diastereomers are probably in all cases more stable, but with energy differences decreasing in the order **4a** > **4b,c** > **4d**.

Regardless, kinetic selectivities can be appreciable, as with **4a,b** in Scheme 1 (>99–88:<1–12 *SR,RS/SS,RR*). In contrast, the higher temperature route to **4a** in eq iii of Scheme 4 is much less diastereoselective. The syntheses of dirhenium complexes **7** and **8** in Chart 1 are highly diastereoselective (90:10, >99:<1), as rationalized by detailed transition state models elsewhere.^{10,23} However, the C_4 complex **11d**, which is prepared by the oxidative coupling of $(\eta^5-C_5Me_5)Re(NO)(PPh_3)(C\equiv CH)$ and has a rhenium–rhenium distance of 7.8288(4) Å, forms as a 50:50 diastereomer mixture.^{8c}

The cyanide bridges in **4a–d** are clearly of high kinetic stability, with no evidence for equilibration with triflate complexes **1a,b**. Since the latter are configurationally labile, this precludes one obvious means of diastereomer interconversion. The triflate complexes could form either by (1) spontaneous dissociation of a rhenium fragment $I-Me_x$ and subsequent addition of triflate ion or (2) direct displacement of the cyanide nitrogen by triflate ion. Extensive studies have shown that **I** is a very high energy intermediate.²⁸ Hence, the former mechanism should be disfavored. Furthermore, Lewis base adducts of **I** undergo *associative* substitution and with retention of configuration.²⁸ “Front-side” displacements have been proposed to account for the stereochemistry. Thus, the latter mechanism would require intercalation of a triflate ion between two bulky rhenium moieties.

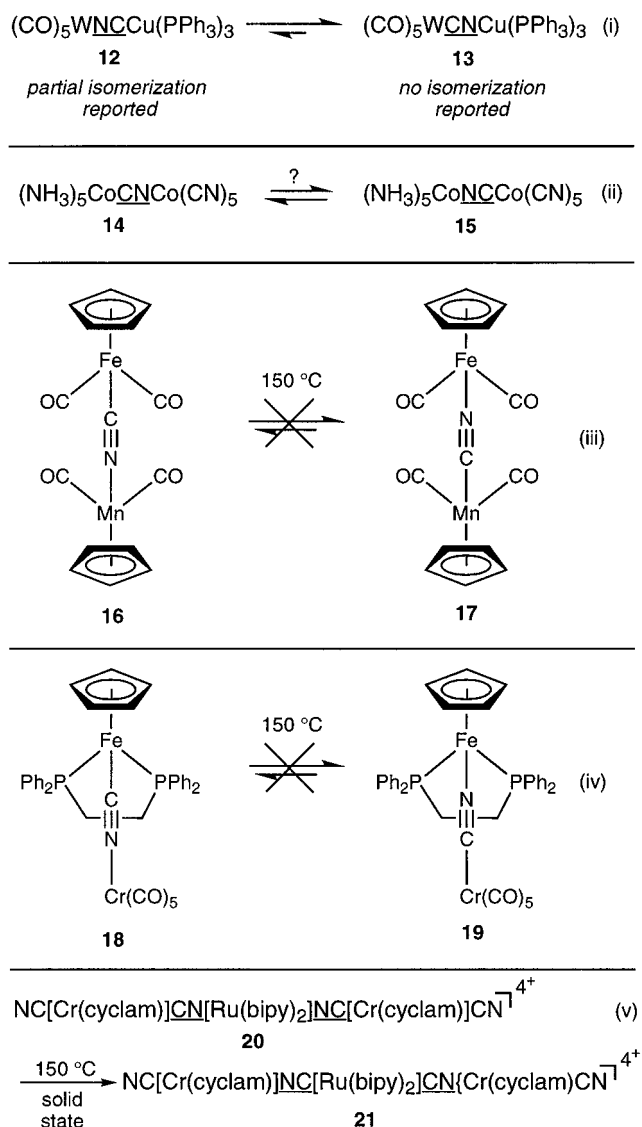
There are only a few other cases where both linkage isomers of an unsymmetrically substituted bridging cyanide complex have been isolated. First, the tungsten/copper complexes **12** and **13** in eq i of Scheme 5 have been independently synthesized.^{1b} Partial isomerization of the former was observed by NMR below room temperature. The dicobalt complexes **14** and **15** (eq ii, Scheme 5) have been crystallographically characterized, but equilibrations have not to our knowledge been attempted.^{6a} The cyclopentadienyl iron/manganese complexes **16** and **17** constitute the closest relatives to **4b,c** and the related iron/chromium complexes **18** and **19** have been reported (eqs iii and iv, Scheme 5).^{6b} None of these could be interconverted below their decomposition points of approximately 150 °C. Interestingly, the ruthenium/dichromium complex **20**, which contains two bridging cyanide ligands, undergoes a double linkage isomerization in the solid state at 150 °C.^{6c}

The linkage isomerization of bridging cyanide ligands could involve a variety of dissociative and nondissociative mechanisms. The data in Scheme 5, together with ours, suggest that none of these are particularly facile processes. Interestingly, the linkage isomers **16** and **17** give pseudoreversible and reversible one electron oxidations, respectively, that differ by 0.24 V. In contrast, the oxidations of **4b,c** differ by only 0.03 V. This presumably reflects the closer similarity of the endgroups in **4b,c**. Indeed, many IR and NMR properties of **4a–d** suggest strong resonance interactions between the two rheniums that evenly distribute the positive charge (**VIII**, **IX**). Also, **4a–d** exhibit some optical features that have no counterparts in the mononuclear precursors **1a** and **2a** or the acetonitrile complex **5** (Figure 1). However, these are relatively weak.

In summary, this study has made available the first family of bridging cyanide complexes with two chiral metal endgroups. The cyanide bridges are of excep-

(29) (a) Fehlhammer, W. P.; Fritz, M. *Chem. Rev.* **1993**, *93*, 1243. (b) Carvalho, M. F. N. N.; Duarte, M. T.; Galvão, A. M.; Pombeiro, A. J. L. *J. Organomet. Chem.* **1996**, *511*, 163.

(30) Reger, D. L. *Inorg. Chem.* **1975**, *14*, 660.

Scheme 5. Other Bridging Cyanide Complexes for Which Linkage Isomers Are Known


tional kinetic and thermodynamic stabilities and not subject to linkage isomerization. These properties suggest that higher (C≡C)_nCN ligands may be of exceptional value as building blocks in the construction of unsaturated, metal-based superlattices, which are receiving intense attention as platforms for nanoelectronic digital circuits.³¹

Experimental Section

General Data. General procedures were given in an earlier paper.^{13b} Solvents were treated as follows: CH₂Cl₂, distilled from CaH₂; hexane, distilled from Na/O=CPh₂; toluene, distilled from Na; pentane, acetone, CH₃CN, CHCl₂CHCl₂, CD₂-Cl₂, CDCl₃, used as received. Reagents were used as received from common commercial sources. Differential scanning calorimetry (DSC) was conducted with a T.A. Instrument Model 2910. Samples (1–3 mg) were loaded in crimped Al pans and heated to 300 °C (5 °C/min) under a nitrogen atmosphere. The *T_c* values were determined using the software program Universal Analysis.³²

(*η*⁵-C₅Me₅)Re(NO)(PPh₃)(OTf) (**1b**). A Schlenk tube was charged with (*η*⁵-C₅Me₅)Re(NO)(PPh₃)(CH₃) (**3b**;¹⁷ 1.200 g,

(31) Andres, R. P.; Bielefeld, J. D.; Henderson, J. I.; Janes, D. B.; Kolagunta, V. R.; Kubiak, C. P.; Mahoney, W. J.; Osifchin, R. G. *Science* **1996**, *273*, 1690.

1.894 mmol) and toluene (20 mL) and cooled to –80 °C (acetone/CO₂). Then HOTf (0.168 mL, 1.89 mmol) was added with stirring, and the cold bath was removed. After 2 h, the red powder was collected by filtration, washed with pentane, and dried by oil pump vacuum to give **1b** (1.10 g, 1.43 mmol, 76%), mp 219–220 °C dec. Anal. Calcd for C₂₉H₃₀F₃NO₄-PReS: C, 45.66; H, 3.96. Found: C, 45.37; H, 4.05. IR (cm⁻¹, KBr/thin film): ν_{NO} 1663/1667 (vs). NMR spectra showed a 3% impurity (¹H, δ 1.79 (CDCl₃); ³¹P, 23.1/23.4 ppm (CDCl₃/CH₂Cl₂), which in view of the correct analysis may be an isomeric species.

NMR:³³ ¹H (δ , CDCl₃) 7.45–7.37 (m, 3Ph), 1.68 (s, C₅Me₅); ¹³C{¹H} (ppm, CDCl₃) 133.8 (d, ²J_{CP} = 10.7, *o*-Ph), 132.6 (d, ¹J_{CP} = 50.8, *i*-Ph), 130.5 (s, *p*-Ph), 128.6 (d, ³J_{CP} = 9.8, *m*-Ph), 116.6 (q, ¹J_{CF} = 318, CF₃), 101.0 (s, C₅Me₅), 10.3 (s, C₅Me₅); ³¹P{¹H} (ppm) 20.2 (s, CDCl₃), 20.0 (s, CH₂Cl₂).

[(*η*⁵-C₅H₅)Re(NO)(PPh₃)CN(PPh₃)(ON)Re(*η*⁵-C₅H₅)]⁺TfO⁻ (**4a**). **Method A.** A Schlenk flask was charged with (*η*⁵-C₅H₅)Re(NO)(PPh₃)(CH₃) (**3a**;³⁴ 0.144 g, 0.258 mmol) and toluene (20 mL) and cooled to –45 °C (acetonitrile/CO₂). Then HOTf (0.023 mL, 0.258 mmol) was added dropwise with stirring to generate (*η*⁵-C₅H₅)Re(NO)(PPh₃)(OTf) (**1a**).^{12,13} After 10 min, solid (*η*⁵-C₅H₅)Re(NO)(PPh₃)(CN) (**2a**;¹⁴ 0.147 g, 0.258 mmol) was added and the cold bath removed. After 14 h, hexane (200 mL) was added to the heterogeneous sample. The orange-yellow powder was collected by filtration, washed with pentane, and dried by oil pump vacuum to give spectroscopically pure **4a** (0.297 g, 0.235 mmol, 91%; >99:<1 *SR,RS/SS,RR*). A portion was crystallized (CH₂Cl₂/hexane, vapor diffusion) to give red-orange prisms, mp (DSC) 247 °C.³² Anal. Calcd for C₄₈H₄₀F₃N₃O₅P₂Re₂S: C, 45.67; H, 3.19. Found: C, 45.60; H, 3.21. IR: see Table 1. UV-vis: 310 nm (6300) sh.³⁵

NMR (*SR,RS*):³³ ¹H (δ , CDCl₃) 7.57–7.41 (m, 18 H of 6Ph), 7.38–7.14 (m, 12 H of 6Ph), 5.06, 5.05 (2s, C₅H₅); ¹³C{¹H} (ppm, CDCl₃) 149.5 (d, ²J_{CP} = 11.4, CN), 134.1, 133.5 (2d, ¹J_{CP} = 56.8, 55.2, *i*-Ph), 133.5, 133.3 (2d, ²J_{CP} = 10.9, 10.9, *o*-Ph), 131.6, 131.5 (2d, ⁴J_{CP} = 2.3, 2.3, *p*-Ph), 129.2 (d, ³J_{CP} = 10.8, *m*-Ph),^{36a} 121.2 (q, ¹J_{CF} = 321, CF₃), 91.7, 91.3 (2s, C₅H₅); ³¹P{¹H} (ppm) 16.8, 16.7 (2s, CDCl₃), 16.64, 16.58 (2s, CH₂Cl₂), 18.1, 17.4 (2s, CH₂Cl₂, –80 °C), 18.2, 17.3 (2s, CH₂Cl₂, –100 °C), 16.5, 16.4 (2s, CHCl₂CHCl₂).

Method B. A 5-mm NMR tube was charged with **1a** (0.018 g, 0.026 mmol)¹² and **2a** (0.015 g, 0.026 mmol) and capped with a septum. Then CH₂Cl₂ (0.8 mL) was added. The tube was kept in a 40 °C bath for 12 h. A ³¹P{¹H} NMR spectrum of the red-orange solution showed only (*SR,RS*)-**4a** (16.7, 16.6 ppm, 2s, 1:1).

Method C. Configurationally labile (*S*)-**1a** was isolated from the reaction of (*R*)-(*η*⁵-C₅H₅)Re(NO)(PPh₃)(CH₃) (97% ee)³⁴ and HOTf as described earlier.¹² A 5 mm NMR tube was charged with (*S*)-**1a** (0.018 g, 0.026 mmol) and (*R*)-**2a** (0.015 g, 0.026 mmol, >98% ee),^{13a,b} capped with a septum, and cooled to –45 °C. Then CDCl₃ (0.8 mL) was added, and the cold bath was allowed to warm. After 12 h, a ³¹P{¹H} NMR spectrum showed peaks for (*RR*)-**4a** at 16.4 and 16.5 (86%) and (*SR*)-**4a** at 16.7 and 16.8 (14%).

Method D. A Schlenk flask was charged with (*S*)-**1a** (0.130 g, 0.187 mmol) and toluene (20 mL) and cooled to –45 °C. Then

(32) Cammenga, H. K.; Epple, M. *Angew. Chem., Int. Ed. Engl.* **1995**, *34*, 1171.

(33) Unless noted otherwise, NMR spectra were recorded at ambient probe temperature and referenced as follows: ¹H, Si(CH₃)₄ (δ 0.00), CHDCl₂ (δ 5.32); ¹³C, CDCl₃ (77.0 ppm), CD₂Cl₂ (53.8 ppm); ³¹P, external 85% H₃PO₄ (0.00 ppm); ¹⁹F, CFCl₃ (0.00 ppm). All coupling constants (*J*) are in Hertz. Only partial NMR data are available for the minor *SS,RR* diastereomers of **4b–d**. When signals are detected, they are separated from those of the *SR,RS* diastereomers by slashes (/).

(34) Agbossou, F.; O'Connor, E. J.; Garner, C. M.; Quirós Méndez, N.; Fernández, J. M.; Patton, A. T.; Ramsden, J. A.; Gladysz, J. A. *Inorg. Synth.* **1992**, *29*, 211.

(35) 2.3–2.5 × 10⁻⁵ M CH₃CN (ϵ , M⁻¹ cm⁻¹).

(36) (a) Only one *m*-Ph signal was observed. (b) Only one *i*-Ph signal was observed. (c) The *i*-Ph signals were not observed. (d) The two PPh₃ ligands gave one signal.

solid (*R*)-**2a** (0.107 g, 0.187 mmol) was added, and the cold bath was removed. After 1 h, hexane (25 mL) was added to the heterogeneous sample. The orange-yellow powder was collected by filtration, washed with pentane, and dried by oil pump vacuum to give **4a** (0.201 g, 0.235 mmol, 85%; 89:11 *RR/SR*). IR: see Table 1.

NMR (*RR*, CDCl₃):³³ ¹H (δ) 7.57–7.41 (m, 18 H of 6Ph), 7.38–7.14 (m, 12 H of 6Ph), 5.07, 5.06 (2s, C₅H₅); ¹³C{¹H} (ppm) 148.4 (d, ²J_{CP} = 11.3, CN), 133.4, 130.0 (2d, ¹J_{CP} = 56.7, 54.9, *i*-Ph), 133.4, 133.2 (2d, ²J_{CP} = 10.8, 11.1, *o*-Ph), 131.3, 131.3 (2d, ⁴J_{CP} = 2.3, 2.3, *p*-Ph), 129.0 (d, ³J_{CP} = 10.3, *m*-Ph),^{36a} 120.8 (q, ¹J_{CF} = 321, CF₃), 91.3, 90.7 (2s, C₅H₅); ³¹P{¹H} (ppm) 16.5, 16.4 (2s).

Method E. A Schlenk flask was charged with [(η⁵-C₅H₅)Re(NO)(PPh₃)(S(CH₂CH=CH₂)₂)]⁺ TfO⁻ (**9**;²⁷ 0.042 g, 0.051 mmol), **2a** (0.029 g, 0.051 mmol), and CH₂Cl₂CHCl₂ (2.0 mL) and kept at 96 °C for 8 h. A black suspension formed. ³¹P{¹H} NMR (ppm, aliquot): 20.6, 16.4, 16.3, 16.1, 16.0, 11.2 (6:20:19:17:19:19). Solvent was removed by oil pump vacuum, and CDCl₃ (1 mL) was added. The sample was filtered through glass wool into a NMR tube. ¹H NMR: δ 5.67 (**9**, 20%), 5.37 (10%), 5.34 (7%), 5.06 (*SR,RS*) and (*SS,RR*)-**4a**, 63%). ³¹P{¹H} NMR: 21.4 (6%), 16.8 (20%, (*SR,RS*)-**4a**), 16.6 (19%, (*SR,RS*)-**4a**), 16.5 (17%, (*SS,RR*)-**4a**), 16.4 (19%, (*SS,RR*)-**4a**), 12.0 (**9**, 19%) ppm. Solvent was removed by rotary evaporation. IR (cm⁻¹, CH₂Cl₂): ν_{CN} 2092 (s), ν_{NO} 1701 (s). These bands are between those of (*SR,RS*)- and (*RR*)-**4a** (Table 1).

Method F. A flask was charged with (*SR,RS*)-**4a** (0.140 g, 0.111 mmol), NH₄⁺ PF₆⁻ (0.091 g, 0.554 mmol), and acetone (100 mL). The mixture was stirred for 1 h and filtered through silica gel. Solvent was removed by rotary evaporation. Then CH₂Cl₂ (100 mL) was added, and the mixture was filtered through Celite. Hexane (150 mL) was added to the filtrate, and the bright orange precipitate was collected on a frit, washed with hexane, and dried by oil pump vacuum to give the hexafluorophosphate salt analogous to (*SR,RS*)-**4a** (0.111g, 0.088 mmol, 80%). The ¹⁹F NMR and IR spectra indicated that anion metathesis was complete. IR (cm⁻¹, CH₂Cl₂): ν_{CN} 2100 (s), ν_{NO} 1695 (vs), ν_{PF} 847 (vs). NMR (CD₂Cl₂):³³ ¹H (δ) 7.61–7.46 (m, 18 H of 6Ph), 7.45–7.32 (m, 12 H of 6Ph), 5.01 (s, 2C₅H₅); ³¹P{¹H} (ppm) 16.7, 16.6 (2s); ¹⁹F (ppm) 105.1 (d, ¹J_{FP} = 708).

[(η⁵-C₅Me₅)Re(NO)(PPh₃)CN(Ph₃P)(ON)Re(η⁵-C₅H₅)]⁺ TfO⁻ (**4b**). **Method A.** Complex **3a** (0.128 g, 0.230 mmol), toluene (60 mL), HOTf (0.020 mL, 0.230 mmol), and (η⁵-C₅Me₅)Re(NO)(PPh₃)CN (**2b**;¹⁶ 0.148 g, 0.230 mmol) were combined in a procedure analogous to that for **4a**. After 36 h, hexane (100 mL) was added and the yellow powder collected by filtration, washed with pentane, and dried by oil pump vacuum to give spectroscopically pure **4b** (0.262 g, 0.197 mmol, 86%; 99:1 *SR,RS/SS,RR*). A portion was crystallized (CH₂-Cl₂/hexane, vapor diffusion) to give orange prisms, mp 233–235 °C dec, DSC T_i/T_d/T_p 230/258/270 °C.³² Anal. Calcd for C₅₃H₅₀F₃N₃O₅P₂Re₂S: C, 47.78; H, 3.78. Found: C, 47.52; H, 3.83. IR: see Table 1. UV–vis: 302 nm (9100) sh.³⁵

NMR (*SR,RS/SS,RR*):³³ ¹H (δ, CDCl₃) 7.59–7.36 (m, 18 H of 6Ph), 7.36–7.15 (m, 12 H of 6Ph), 5.00/5.11 (2s, C₅H₅), 1.77/1.64 (2s, C₅Me₅); ¹³C{¹H} (ppm, CDCl₃) 159.1 (d, ²J_{CP} = 10.9, CN), 133.3, 133.2 (2d, ²J_{CP} = 10.9, 10.4, *o*-Ph), 133.1 (d, ¹J_{CP} = 55.5, *i*-Ph),^{36b} 131.4, 131.2 (2d, ⁴J_{CP} = 2.1, 2.1, *p*-Ph), 128.8, 128.7 (d, ³J_{CP} = 10.9, 10.4, *m*-Ph), 120.9 (q, ¹J_{CF} = 321, CF₃), 101.9/101.7 (2s, C₅Me₅), 91.7/91.4 (2s, C₅H₅), 9.9/9.7 (2s, C₅Me₅); ³¹P{¹H} (ppm) 18.9/18.7, 16.0/15.8 (4s, CDCl₃), 18.9, 16.0 (2s, CH₂Cl₂), 20.1, 16.3 (2s, CH₂Cl₂, –80 °C), 20.6, 16.1 (2s, CH₂Cl₂, –100 °C).

Method B. Complex **1a** (0.015 g, 0.023 mmol), **2b** (0.016 g, 0.023 mmol), and CH₂Cl₂ (0.8 mL) were combined in an NMR tube as described for **4a**. ³¹P{¹H} NMR (ppm, *SR,RS/SS,RR*): 19.0/18.9, 16.0/15.8 (4s, 2 × 88:12).

(37) This value is recommended for standardizing data from the solvent/electrolyte combination employed to a SCE reference, see: Connelly, N. G.; Geiger, W. E. *Chem. Rev.* **1996**, *96*, 877.

[(η⁵-C₅H₅)Re(NO)(PPh₃)CN(Ph₃P)(ON)Re(η⁵-C₅Me₅)]⁺ TfO⁻ (**4c**). **Method A.** Complex **3b** (0.072 g, 0.115 mmol), toluene (10 mL), HOTf (0.011 mL, 0.126 mmol), and **2a** (0.066 g, 0.115 mmol) were combined in a procedure analogous to that for **4a**. After 12 h, hexane (50 mL) was added and the tan powder collected by filtration, washed with pentane, and dried by oil pump vacuum to give spectroscopically pure **4c** (0.129 g, 0.097 mmol, 84%; 95:5 *SR,RS/SS,RR*). A portion was crystallized (CH₂Cl₂/hexane, vapor diffusion) to give orange prisms, mp 235–237 °C dec. DSC (88:12 *SR,RS/SS,RR*) T_i/T_d/T_p 224/233/247 °C.³² Anal. Calcd for C₅₃H₅₀F₃N₃O₅P₂Re₂S: C, 47.78; H, 3.78. Found: C, 47.59; H, 3.80. IR: see Table 1. UV–vis: 310 nm (7700) sh.³⁵

NMR (*SR,RS/SS,RR*):³³ ¹H (δ, CDCl₃) 7.61–7.36 (m, 18 H of 6Ph), 7.36–7.10 (m, 12 H of 6Ph), 4.98/5.10 (2s, C₅H₅), 1.68/1.55 (2s, C₅Me₅); ¹³C{¹H} (ppm, CDCl₃) 149.2 (d, ²J_{CP} = 10.9, CN), 133.7 (d, ¹J_{CP} = 57.1, *i*-Ph),^{36b} 133.4, 133.1 (2d, ²J_{CP} = 10.9, 10.9, *o*-Ph), 131.5, 131.1 (2d, ⁴J_{CP} = 2.1, 2.1, *p*-Ph), 128.9, 128.8 (2d, ³J_{CP} = 10.9, 10.4, *m*-Ph), 120.9 (q, ¹J_{CF} = 321, CF₃), 101.6/101.4 (2s, C₅Me₅), 91.2/90.9 (2s, C₅H₅), 9.7/7.3 (2s, C₅Me₅); ³¹P{¹H} (ppm) 17.8/17.5, 15.9/16.3 (4s, CDCl₃), 17.8/17.4, 15.7/16.2 (4s, CH₂Cl₂), 18.5/17.8, 16.3/16.5 (4s, CH₂Cl₂, –80 °C), 18.8/18.4, 16.4/15.9 (4s, CH₂Cl₂, –100 °C).

Method B. Complex **1b** (0.020 g, 0.026 mmol), **2a** (0.015 g, 0.026 mmol), and CH₂Cl₂ (0.8 mL) were combined in an NMR tube as described for **4a**. ³¹P{¹H} NMR (ppm, *SR,RS/SS,RR*): 17.9/17.4, 15.7/16.2 (4s, 2 × 66:34).

[(η⁵-C₅Me₅)Re(NO)(PPh₃)CN(Ph₃P)(ON)Re(η⁵-C₅Me₅)]⁺ TfO⁻ (**4d**). **Method A.** Complex **3b** (0.204 g, 0.323 mmol), toluene (40 mL), HOTf (0.0290 mL, 0.323 mmol), and **2b** (0.208 g, 0.323 mmol) were combined in a procedure analogous to that for **4a**. The mixture was kept at 50 °C for 12 h and room temperature for 24 h. The orange powder was collected by filtration, washed with pentane, and dried by oil pump vacuum to give spectroscopically pure **4d** (0.323 g, 0.230 mmol, 71%; 71:29 *SR,RS/SS,RR*). Portions were crystallized (CH₂Cl₂/hexane, vapor diffusion) to give deep red prisms (95–98:5–2 *SR,RS/SS,RR*), DSC T_i/T_d/T_p 222/239/270 °C.³² Anal. Calcd for C₅₈H₆₀F₃N₃O₅P₂Re₂S: C, 49.67; H, 4.31. Found: C, 49.40; H, 4.22. IR: see Table 1. UV–vis: 312 nm (6900) sh.³⁵ MS (+)-FAB, 5 kV, Ar, 3-Nitrobenzyl alcohol/CH₂Cl₂ matrix; *m/z* for most intense peak of isotope envelope): 1252 ([η⁵-C₅Me₅)Re(NO)(PPh₃)CN(Ph₃P)(ON)Re(η⁵-C₅Me₅)]⁺, 100), 990 (1252–PPh₃, 50), 640 ([η⁵-C₅Me₅)Re(NO)(PPh₃)CN)]⁺, 10), 614 ([η⁵-C₅Me₅)Re(NO)(PPh₃)]⁺, 24).

NMR (*SR,RS/SS,RR*):³³ ¹H (δ, CDCl₃) 7.58–7.32 (18H of 6Ph), 7.32–7.18 (12H of 6Ph), 1.50/1.71, 1.58/1.60 (4s, C₅Me₅); ¹³C{¹H} (ppm, CDCl₃) 157.3 (d, ²J_{CP} = 10.6, CN), 133.6, 133.5 (2d, ²J_{CP} = 11.2, 11.2, *o*-Ph),^{36c} 131.3, 131.2 (2d, ⁴J_{CP} = 2.3, 2.3, *p*-Ph), 128.9, 128.9 (2d, ³J_{CP} = 10.9, 10.4, *m*-Ph), 120.8 (q, ¹J_{CF} = 321, CF₃), 101.8/101.6, 101.5/101.2 (4s, C₅Me₅), 10.0/9.5, 9.8/9.4 (4s, C₅Me₅); ³¹P{¹H} (ppm) 19.2/17.9, 17.5/17.9 (3s, CDCl₃), 19.3/17.8, 17.5/17.8 (3s, CH₂Cl₂), 20.2/18.5, 17.5/18.5 (3s, CH₂Cl₂, –80 °C), 20.3/18.6, 17.3/18.6 (3s, CH₂Cl₂, –100 °C).^{36d}

Method B. Complex **1b** (0.018 g, 0.023 mmol), **2b** (0.015 g, 0.023 mmol), and CH₂Cl₂ (0.8 mL) were combined in an NMR tube as described for **4a**. ³¹P{¹H} NMR (ppm, *SR,RS/SS,RR*): 19.3, 17.8, 17.6 (3 s, 60:(40 + 40):60).^{36d}

Cyclic Voltammetry. All experiments utilized a EG & G Princeton Applied Research Model 273 potentiostat (PARC 4.0 software) and CH₂Cl₂ solutions (freshly distilled and N₂

(38) Frenz, B. A. The Enraf-Nonius CAD 4 SDP – A Real-time System for Concurrent X-ray Data Collection and Crystal Structure Determination. In *Computing and Crystallography*; Schenk, H., Olthoff-Hazelkamp, R., van Koningsveld, H., Bassi, G. C., Eds.; Delft University Press: Delft, Holland, 1978; pp 64–71.

(39) Sheldrick, G. M. *SHELXL-93, Program for Crystal Structure Refinement*; University of Göttingen: Göttingen, Germany, 1993.

(40) Cromer, D. T.; Waber, J. T. In *International Tables for X-ray Crystallography*; Ibers, J. A., Hamilton, W. C., Eds.; Kynoch: Birmingham, England, 1974; Vol. IV, pp 72–98, 149–150; Tables 2.2B and 2.3.1.

purged) that were $7\text{--}8 \times 10^{-3}$ M in **4a–d** and 0.1 M in $n\text{-Bu}_4\text{N}^+ \text{BF}_4^-$ (recrystallized and dried under vacuum at 75 °C, 24 h). Cells were fitted with Pt working (1.6 mm diameter) and counter electrodes and a Ag wire pseudoreference electrode. Ferrocene was subsequently added ($E^\circ + 0.46$ V)³⁷ and calibration voltammograms recorded.

Crystallography. Data were collected on red-orange prisms of (*SR,RS*)-**4a** (above) as outlined in Table 2. Cell constants were obtained from 25 reflections with $10^\circ < 2\theta < 20^\circ$. The space group was determined from systematic absences ($h0l$ $h + l = 2n + 1$, $0k0$ $k = 2n + 1$) and subsequent least-squares refinement. Lorentz, polarization, and empirical absorption (ψ scans) corrections were applied. The structure was solved by standard heavy-atom techniques with the Molen-VAX package³⁸ and refined with SHELXL-93.³⁹ Non-

hydrogen atoms were refined with anisotropic thermal parameters. The ReCNRe carbon and nitrogen atoms were assigned based upon the orientation that refined better. Hydrogen atom positions were calculated, added to the structure factor calculations, and refined (riding model). Scattering factors and Δf and $\Delta f'$ values were taken from the literature.⁴⁰

Acknowledgment. We thank the Department of Energy for support of this research.

Supporting Information Available: Tables of atomic coordinates and anisotropic thermal parameters for **4a** (4 pages). Ordering information is given on any current masthead page.

OM970167+